



Influence of the Transverse Inhomogeneity on the Nonlinear Post-Buckling Path of Compressed FG Cylindrical Panels

Olga LYKHACHOVA¹⁾, Zbigniew KOŁAKOWSKI²⁾

¹⁾ *Department of Structural Mechanics and Strength of Materials
Prydniprowska State Academy of Civil Engineering and Architecture*

Dnipro, Ukraine
e-mail: lykhachova.olga@gmail.com

²⁾ *Department of Strength of Materials
Lodz University of Technology*

Lodz, Poland
e-mail: zbigniew.kolakowski@gmail.com

In this paper, nonlinear stability of axially compressed cylindrical panels simply supported according to two types of boundary conditions (with possible or limited circumferential displacements of unloaded sides) is presented. Panels made of functionally graded materials (FGMs) of two constituents (metallic and ceramic phases) are treated as multi-layered composite structures with transverse inhomogeneity. Volume fractions of ceramics and metal distribution throughout the layer thickness are described by a simple power law. The influence of the transverse inhomogeneity of FGM panels on unsymmetrical stable post-buckling paths is shown. Special attention is paid to effect of the imperfection sign on post-buckling paths of investigated FGM panels. Some validations of the finite element analysis are discussed for isotropic panels compressed according to two (force and kinematic) loading schemes.

Key words: cylindrical panel, FGM, post-buckling path, transverse inhomogeneity, axial compression, boundary conditions, loading schemes.

NOTATIONS

- a – unloaded axial dimension of a panel,
- A, B, D – extensional, coupling and bending stiffness matrices,
- b – loaded circumferential dimension of a panel,
- E, E_m, E_c – Young's moduli of an isotropic material, metal and ceramics,
- k – curvature parameter,
- N, M – stress and moment resultants,
- N_{cr} – critical load,

- p – intensity of axial compression,
 q – volume fraction exponent (i.e., for $q = 0$ – panel is fully ceramic and for $q = \infty$ – panel is metallic),
 R – panel radius,
 rot x , rot y , rot z – possible rotations about corresponding coordinates x , y , z ,
 t – panel thickness,
 ux , uy , uz – possible displacements along corresponding coordinates x , y , z ,
 V_m , V_c – volume fractions of metal and ceramics,
 w – panel deflection (along coordinate x),
 w^* – initial imperfection,
 x , y , z – radial, circumferential and axial coordinates in the cylindrical coordinate system,
 ε_x , ε_y , ε_{xy} – extension deformations,
 κ_x , κ_y , κ_{xy} – bending deformations,
 ν , ν_m , ν_c – Poisson's ratio of an isotropic material, metal and ceramics.

1. INTRODUCTION

In the 1980s, the concept of heterogeneous material resistant to high temperatures was first presented. This was functionally graded material (FGM) in which the material properties are gradually changing along the thickness direction. In the beginning of twenty-first century, we have witnessed a particularly intensive development of research on the structures made of FGMs. BIRMAN and BYRD [1] presented the state-of-the-art review of the principle developments in modelling and analyses of functionally graded (FG) structures in the first decade of the twenty-first century. LIEW *et al.* [2] reviewed different types of finite element analyses. JHA *et al.* [3] presented a review of the papers on thermoelasticity and vibration of FGM structures. In 2015, the latest to date review was presented by SWAMINATHAN *et al.* [4], in which authors discussed various methods of analysis used for the stress, vibration and buckling of FGM structures under different types of mechanical and/or thermal loads. In their study, the thin-walled columns and/or beams consisting of plate elements are subjected to different static loads and can buckle in different modes from global (i.e., flexural, flexural-torsional, lateral, distortional) to local and the coupled buckling modes. The length of column is the most important. If a column is short, the local mode is the lowest mode and local buckling takes place. For a long column, the global buckling mode is the lowest mode.

The eigenvalue problem of FGM structures under mechanical load can be solved using the analytical methods based on the three-dimensional elasticity theory and the two-dimensional elasticity theory or the finite element method (FEM). The buckling loads and modes are found in FGM structures under vari-

ous boundary and loading conditions. BIRMAN [5] was the first to solve the eigenvalue problem of FGM plates under mechanical loads. MA and WANG [6] compared the solutions of buckling problem obtained using the first-order (FSDT), third-order (TSDT), and classical (CPT) plate theories. The first-order plate theory (FSDT) is sufficient to consider the buckling of FGM structures. MOHAMMADI *et al.* [7] presented some solutions for a buckling problem of thin FGM plates based on the classical plate theories subjected to different mechanical loads under various boundary conditions. The pre-buckling state of FGM plates based on the Mindlin theory was discussed by NADERI and SAIDI [8]. The eigenvalue problem of the FGM structures under mechanical load using FEM was investigated by BATENI *et al.* [9], NAEI *et al.* [10], LEE and KIM [11] and many more.

Post-buckling states were obtained using an analytical numerical method by YANG and SHEN [12]. Authors used perturbation to investigate the post-buckling behaviour of the clamped FGM rectangular plates based on the CPT under transverse and in-plane loads, and presented some unique characteristics of structures made of FGM composite. YANG *et al.* [13] studied the influence of initial imperfection on the post-buckling behaviour of FGM plates based on the first-order plate theory (FSDT) under various boundary conditions. In their study, it was shown that imperfections of FGM structures are much less important in comparison to isotropic material structures. The FEM approach was also used to determine the post-buckling behaviour of FGM structures by LEE and KIM [11]. More results for the nonlinear post-buckling analysis of this type of elements under different types of loads are shown in the monograph by HUI-SHEN [14].

FGMs are still a relatively new class of composite materials used in numerous engineering applications. A standard FGM is an inhomogeneous composite made of two constituents – typically metallic and ceramic phases. The combination of ceramics with a metal component renders specific characteristics to FG structures, such as better resistance to high temperature (ceramics) and good mechanical features (metal), which further reduce possibility of the fracture of the whole gradient structure. These features make high temperature environments the leading application area for FG structures. In the case of the FGM layer, volume fractions of ceramics and metal distribution throughout the layer thickness are described by a simple power law. Transverse inhomogeneity of FG panels according to the classical laminate plate theory (CLPT) has a non-trivial coupling matrix B (for more details see Appendix).

In [15], on the basis of Koiter's nonlinear theory of conservatory systems, it was shown that the FG plate structures have unsymmetrical stable post-buckling equilibrium paths. Due to the presence of the transverse inhomogeneity (i.e., equivalent to nontrivial submatrix B), the coupling between extensional and

bending deformations exists. For example, cylindrical isotropic panels subjected to compression have the unsymmetrical stable post-buckling paths.

As it follows from the short review of present state-of-the-art studies concerning composite structures research, there are also some researches [16–22] that deal with post-buckling analyses of compressed panels with various boundary conditions, mostly assuming clamped and/or simple supports. And even such common supports can be realised differently [22], which is not adequately researched at the moment. The same applies to the influence of transverse inhomogeneous real FG panels on the load-deflection response.

In this paper, the influence of the transverse inhomogeneous FG panels on the unsymmetrical stable post-buckling paths of cylindrical panels (i.e., the interactive effects of the two unsymmetrical post-buckling paths) is taken into account for two types of boundary conditions, which is associated with simple support at all edges, and possible or limited circumferential displacements of unloaded sides. Attention is paid to an effect of the imperfection sign (sense), and, therefore, to various post-buckling equilibrium paths of real structures with imperfection. Also, some validations of the finite element analysis are discussed for an isotropic panels compressed according to two different loading schemes [23] (see Sec. 4).

2. FORMULATION OF THE PROBLEM

The commercial ANSYS software is applied in the numerical calculations. In the finite element method solution, FG panels are modelled as multi-layered composite structures [16], whose graded material properties in the range of 10–40 isotropic layers [17] are defined. After the convergence analysis, the model with twenty layers is accepted. For meshing, a shell element (SHELL181 from ANSYS library) is employed with four nodes and six degrees of freedom at each node, and the total number of degrees of freedom is equal to 4056.

The initial imperfections are introduced by updating the finite element mesh with the first mode shape of the eigen-buckling solution, with an assumed magnitude corresponding to the panel thickness. The eigen-buckling analysis determined the critical load in spite of the fact that an eigenmode and analysis of the modes preceded the nonlinear buckling analysis.

Cylindrical shallow panels (Fig. 1) subjected to axial compression along direction z are considered. Axial compression is applied as uniform forces distributed along the curved edges of the panels (force loading, [23]). All panels are subject to Hooke's law. A detailed analysis of the calculations is conducted for thin-walled panels with the following dimensions (Fig. 1): $a = b = 77.5$ mm, $t = 1.0$ mm, $R = 500.0$ mm (thickness parameter – $R/t = 500$). The curvature parameter is $k = b^2/Rt = 12$.

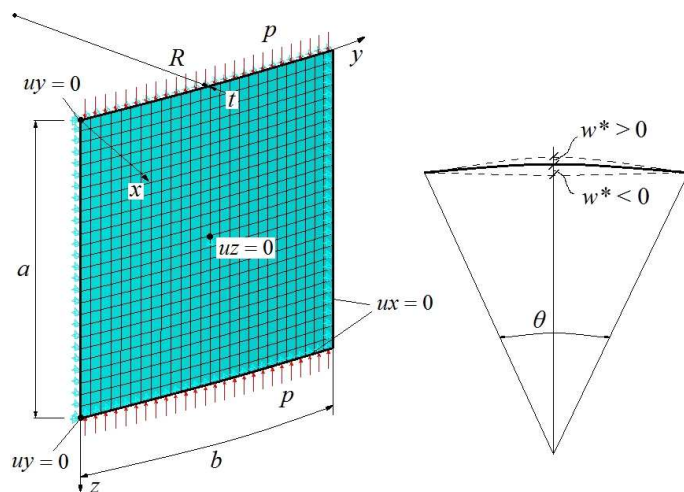


FIG. 1. Cylindrical shallow panels of variant II and III with BCs1.

Two types of boundary conditions are studied (according to ANSYS designation in global cylindrical coordinate system):

- BCs1 – simple support at all edges. As a result, radial displacements $ux = 0$ are at all edges, and in addition, circumferential displacements $uy = 0$ are at two points $(0, 0, 0)$ and $(0, 0, a)$, as well as vertical displacements $uz = 0$ are in the middle of a panel $(0, b/2, a/2)$.
- BCs2 – simple support at loaded edges, where radial displacements $ux = 0$, and hinged support at unloaded edges, where both radial and tangent displacements $ux = uy = 0$, in addition vertical displacements $uz = 0$ are in the middle of a panel $(0, b/2, a/2)$.

The assumed boundary conditions of the first type and the division into finite elements are presented in Fig. 1.

The panels are made of two materials:

- isotropic material (aluminium) with the following material properties: $E = 79.28$ GPa and $\nu = 0.3268$.
- Al-TiC functionally graded material for the fraction exponent (A1) (see Appendix) $q = 1.0$ [15]. The component material properties of Al-TiC functionally graded materials are as follows: for aluminium: $E_m = 69$ GPa, $\nu_m = 0.33$, for TiC: $E_c = 480$ GPa, $\nu_c = 0.20$.

Three variants of the panels are considered, namely:

- variant I – isotropic panel (the so-called reference variant), IP;
- variant II – FG panel (ceramic internal surface of the cross-section, metal – external surface), PCM;

- variant III – FG panel (metal internal surface of the cross-section, external surface made of ceramics), PMC.

The isotropic panel is transverse homogeneous symmetric, whereas the FG panels are transversely inhomogeneous. Two variants of FG structures are assumed, and two cases of manufacturing such panels are possible. The ceramic surface is resistant to high temperatures. Variant II protects the internal surface of the panel against high temperature, whereas variant III protects the external surface.

3. ANALYSIS OF THE RESULTS

As the first stage of the present numerical research, linear solutions have been realised. Table 1 shows critical values for three variants of the considered panels for both types of boundary conditions. Although the material of panels BCs2 provides the level of critical loads about two times higher than BCs1, panels supported by BCs1 have buckling modes (Fig. 2a) with one half-wave outwards the panel centre of curvature for FG structures and inwards in the case of isotropic material. BCs2 impose two half-wave modes (Fig. 2b) for both isotropic and composite materials. Generally, panels made of PMC demonstrate higher level of buckling loads than panels made of PCM, regardless of the type of boundary conditions. This fact can be also observed in the further presented nonlinear analyses (Figs. 3–5).

Table 1. Critical load N_{cr} for three variants of the panel and two schemes of boundary conditions.

Critical load	Schemes of boundary conditions	Variant I – IP	Variant II – PCM	Variant III – PMC
N_{cr} [kN]	BCs1	4.794	13.478	14.110
	BCs2	8.850	24.947	27.765

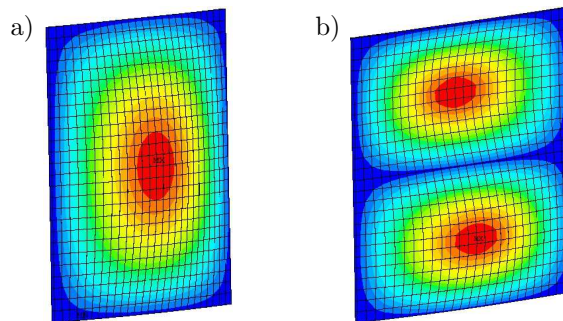


FIG. 2. The eigen-buckling modes and the shape of imperfections: a) BCs1 and b) BCs2.

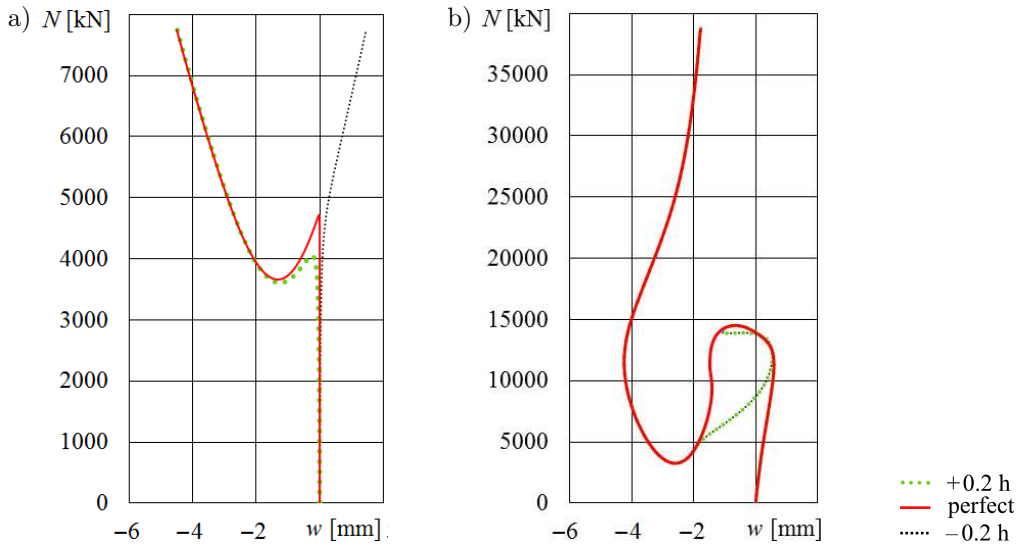


FIG. 3. Isotropic panel IP: a) BCs1 and b) BCs2.

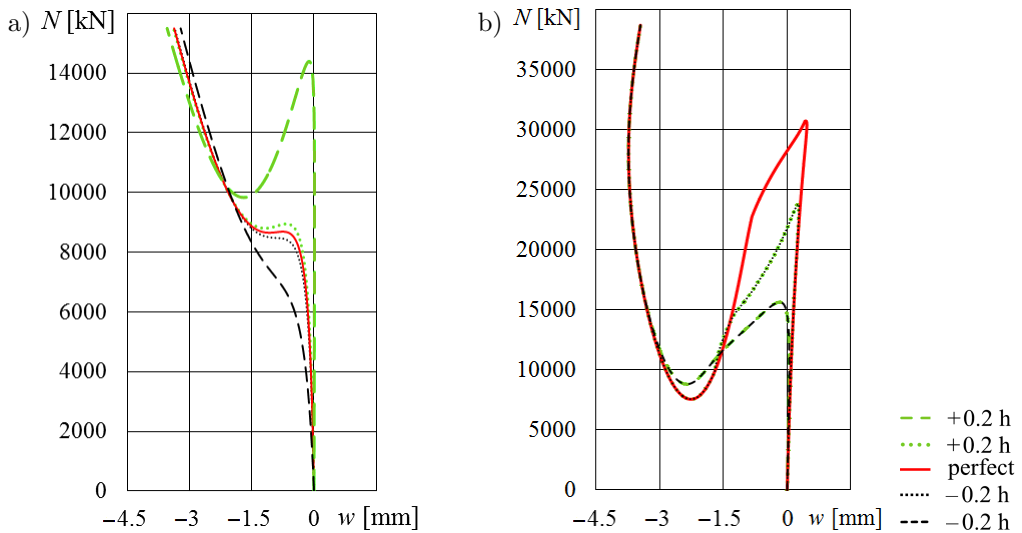


FIG. 4. FG panel PCM: a) BCs1 and b) BCs2.

Post-buckling equilibrium paths for perfect and real panels with imperfections are presented in Figs. 3–5. These figures depict an influence of the external loading on the panel maximal deflection w . Various values of initial imperfections of the FG panels are studied: $w^* = -0.02t, 0.02t, -0.2t$ and $0.2t$. In the case of the isotropic panel (variant I), only the two first values of imperfection

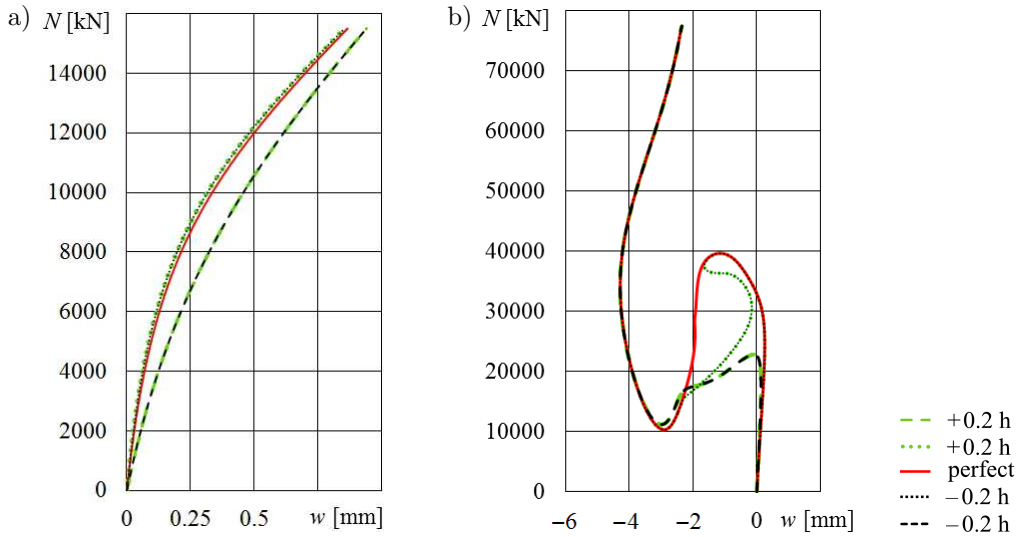


FIG. 5. FG panel PMC: a) BCs1 and b) BCs2.

are considered. The considered signs (senses) of imperfection of composite panels are shown in Fig. 1, accordingly to the used coordinate system.

For isotropic panels with BCs1 (Fig. 3a), one can see that the imperfection w^* sign exerts a considerable influence on different post-buckling equilibrium paths, i.e., on various signs of the deflection w values, which is disclosed by the shape of imperfections (Fig. 2a). This effect can be easily explained [17, 20] by the fact that the coupled submatrix B is different from zero for the FG panels. Similar effects can be also observed for composite panels when the submatrix B is non-zero. Obviously, BCs2 cannot reveal this effect because of the symmetry of imperfections (Fig. 2b) neither for isotropic panels I nor for FG panels II and III (Figs. 4b and 5b).

For the PCM panels with BCs1, the imperfection w^* sign does not affect the deflection w direction towards the panel centre (Fig. 4a). Also for the PMC panels with BCs1 (Fig. 5a), the imperfection w^* sign does not influence the deflection w direction outside the panels. In Fig. 5a, the curves for the imperfection $w^* = -0.2t, 0.2t$ overlap, identically as for $w^* = -0.02t, 0.02t$. As it can be easily observed in Figs. 4a and 5a, the imperfection sign does not affect the displacements w for the PCM and PMC panels. However, the absolute quantity w^* exerts such an influence.

In the case of FG panels with BCs2 (due to the symmetrical shape of imperfections), equilibrium paths are identical and they do not depend on the imperfection sign, however the imperfection magnitude is still important. Let us also note that a general level of buckling loads is higher for BCs2 than for BCs1,

but there is a principal difference between post-buckling equilibrium paths for the two boundary conditions. Panels of all variants with BCs2 have both down-going and up-going branches (Figs. 3b, 4b, 5b), while panels with BCs1 have mostly up-going branches (Figs. 3a, 4a, 5a). Exceptions can be found only at positive imperfections w^* for material of I (isotropic) and II (PCM) variant.

Figure 6 illustrates some typical nonlinear buckling modes of PCM panels at different levels of axial compression for both boundary conditions. The first line

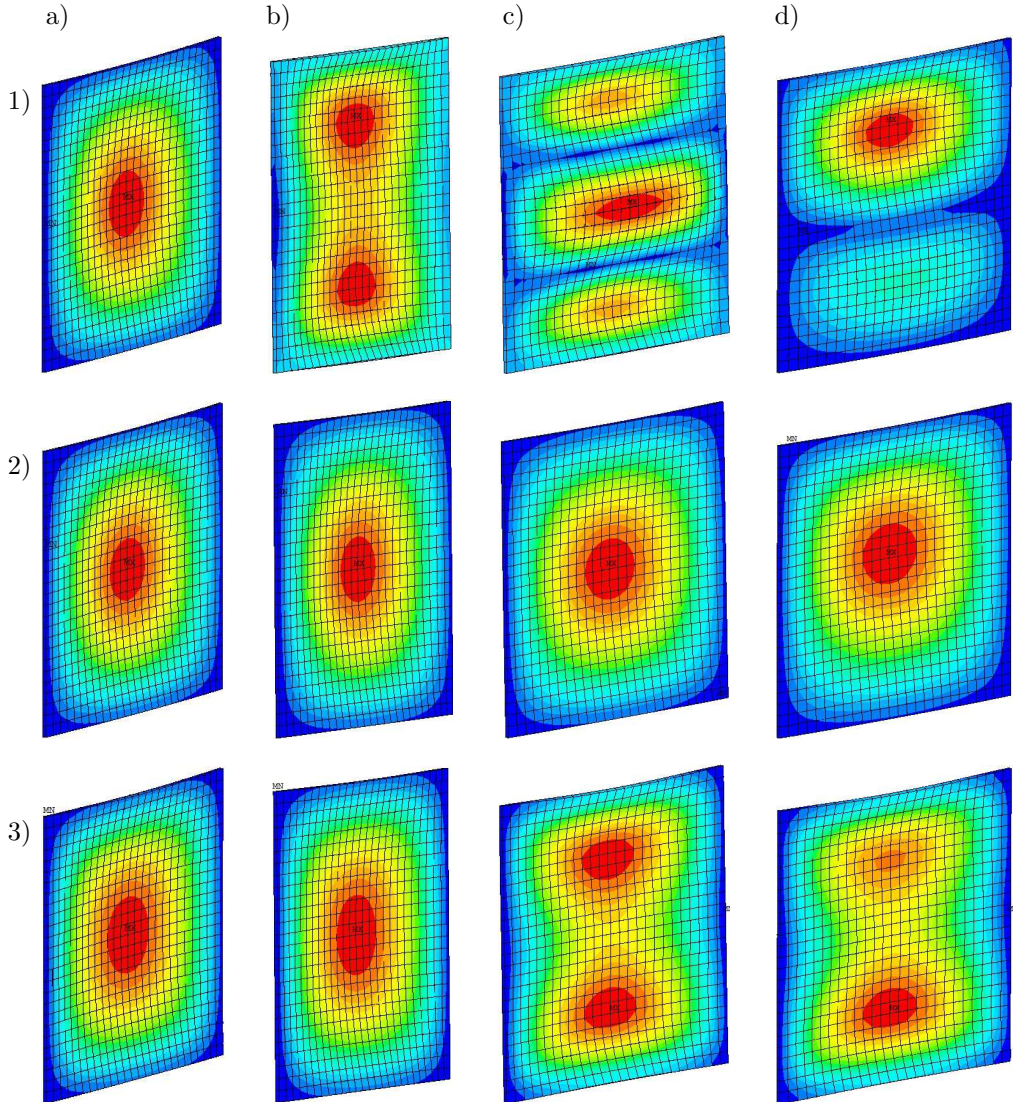


FIG. 6. Nonlinear buckling modes for PCM (variant II) panel BCs1: a) perfect, b) $w^* = 0.2t$ and panel BCs2: c) perfect, d) $w^* = \pm 0.2t$.

of modes corresponds to limit loads (1). If there are no down-going equilibrium branches, load level is chosen according to the same values of the panel deflection. The second line corresponds to lower critical loads (2), and the last line of modes corresponds to the end of loading (3).

Buckling modes of perfect PCM (variant II) panels with BCs1 (Fig. 6a) are the same in the case of PCM panels with imperfections $w^* = -0.2t, \pm 0.02t$. The same is also the case for isotropic panels (variant I perfect and imperfect) and for PMC panels (variant III perfect and imperfect). However, in the last variant of material, the curvature of shapes is outwards the centre of the panels. Relatively high level of the limit load for the PCM panel with $w^* = 0.2t$ (Fig. 4a) is accompanied by a rather complicated mode that is presented in Fig. 6b-1.

Nonlinear buckling modes of PCM (variant II) panels with imperfections $w^* = \pm 0.2t$ (Fig. 6d) keep a linear shape with two half-waves (Fig. 2b). The same behaviour is also characteristic for PCM (variant II) panels with imperfections $w^* = \pm 0.02t$ and for PMC (variant III) panels with imperfections $w^* = \pm 0.2t$.

In the case of BCs2 perfect isotropic (variant I), perfect PMC (variant III) and PMC with imperfections $w^* = \pm 0.02t$, the panels buckle in the same manner as perfect PCM (variant II, Fig. 6c-2 and 6c-3). However, the limit loads for variants I and III are accompanied by buckling modes of inverse deformation (Fig. 6c-1), in which there is a dent in the middle and two buckles at the edges.

Nonlinear buckling modes of PCM (variant II) panels with imperfections $w^* = \pm 0.2t$ (Fig. 6d) keep a linear shape with two half-waves (Fig. 2b). The same behaviour is also specific for PCM (variant II) panels with imperfections $w^* = \pm 0.02t$ and for PMC (variant III) panels with imperfections $w^* = \pm 0.2t$.

4. EFFECT OF LOADING SCHEME

In the previous sections, we have discussed two different types of boundary conditions with assumption of the traditional scheme of a compressive loading. The classical axial compression has been presented as uniform forces distributed along curved edges. Most analytical models use this scheme of loading. However, this is not accomplished in the practice and experiments. Nevertheless, it is still reasonable to model such scheme, as it always appears more or less in the case of real structures loading. Besides, the force loading provides the lowest bound of predicted buckling loads in comparison with kinematic loading [23], which can be applied as uniform displacements distributed along curved edges. The comparison of force and kinematic loadings is insufficiently studied in literature despite the essential effect of both loadings on the panel response and responses of other structures with essentially non-uniform stress-strain state.

In this research, we studied the effect of loading scheme (force or kinematic loading) on post-buckling equilibrium paths for an isotropic cylindrical panel.

Due to the open cross-section geometry of panels the effect of loading scheme was to be discovered. To compare and verify the results of our numerical simulations, we used geometrical and mechanical parameters of panels obtained in [19, 22]. The panels were characterised, according to the previous sections, with thickness parameter $R/t = 462$ and another curvature parameter $k = 27$, $a = 374.65$ mm, $b = 368.3$ mm, $t = 3.3$ mm, and $R = 1524.0$ mm. Material properties referring to aluminium are: $E_m = 68.95$ GPa, and $\nu_m = 0.33$. Boundary conditions (BCs3 in the former designation) are as follows [19, 22]: clamped along the loaded and simply supported along unloaded edges. Therefore, radial displacements $ux = 0$ and rot $y = 0$ at all edges, circumferential displacements $uy = 0$ and rot $z = 0$ along loaded edges, and in addition, vertical displacements $uz = 0$ in the middle of a panel $(0, b/2, a/2)$.

Geometrically linear (bifurcation) and nonlinear analyses of perfect panels and panels with imperfections were performed. Then, the numerical results were validated with solutions presented in [19, 22]. In Fig. 7, we can see responses of central deflection on buckling loads of panels, as well as solutions [19, 22]. Considered loading schemes provide the same qualitative response of panels for different levels of axial loads. Two unlike behaviours of panels can be found in Fig. 7. First one is associated with outward deformations of a panel. The panel has a monotonically increasing stable response, where free expansion of panel edges in the circumferential direction is limited ($uy = 0$). In this case, results of geometrically nonlinear analyses of perfect panels loaded both with kinematic and force compression are in good agreement with a solution [22] found for kinematic loading and prescribed BCs3.

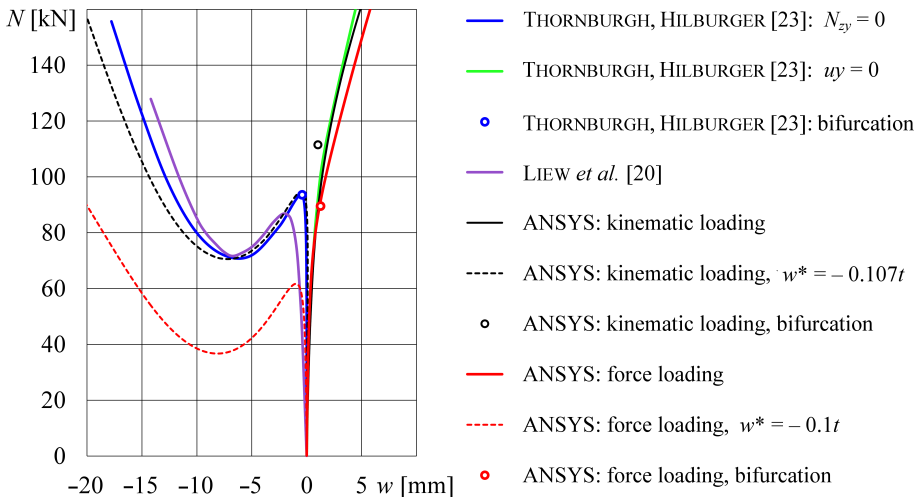


FIG. 7. Comparison of buckling analysis results for compressed aluminum panels with different loading conditions.

The other response of the panel [22] is observed when free expansion of curved loaded edges is possible. In that case, $N_{zy} = 0$ was an input instead of $uy = 0$ and the panel deformed inwards. Although we could not achieve modelling $N_{zy} = 0$ at the loaded edges, we performed calculations of panels with various inward imperfections for both considered schemes of compression. As a result, the difference between the numerical limit load and the solution [22] was reached to be about 1% for the kinematic loading of the panel with imperfections $w^* \sim -0.1t$, while the force loading decreased buckling load at 34% for the same imperfection magnitude. By contrast, linear buckling solution for the force loading provides better agreement with the solution presented in [22] than for the kinematic loading (see Table 2).

Table 2. Comparison of critical load N_{cr} for an aluminium panel with BCs3.

Loads	Schemes of boundary conditions	Schemes of loading	ANSYS	Difference to THORNBURGH, HILBURGER [22]	Difference to LIEW <i>et al.</i> [19]
N_{cr} [kN]	BCs3	kinematic	111.5	20%	22%
		force	89.51	4%	3%

Overall, different schemes of loading allow to accurately enough predict the load-deflection response of isotropic cylindrical panels considered in known solutions and experiments. In the case of perfect panels, differences between schemes are negligible, while in the case of imperfections they are more significant and ought to be taken into account.

5. CONCLUSIONS

In this paper, the influence of the transverse inhomogeneity on post-buckling equilibrium paths of FG cylindrical panels under compression was analysed. This effect is associated with the interaction of two unsymmetrical post-buckling paths for the FG panels.

Numerical analysis of buckling problem of compressed cylindrical panels with imperfections is realised using ANSYS software for three variants of material: isotropic and two FGMs (PMC and PCM), and two types of boundary conditions (BCs1 – simply supported at all edges and BCs2 – simply supported at loaded edges, hinged supported at unloaded edges).

Regardless of the type of boundary conditions, panels made of PMC (ceramics outside) demonstrate a higher level of buckling loads than panels made of PCM (metal outside).

For BCs1 with possible circumferential displacements, the sign of imperfection exerts an influence on the post-buckling equilibrium path of the FG panels.

This effect can be easily explained by the fact that the coupled submatrix B is different from zero for the FG panels. Similar effects can be also observed in composite panels when the submatrix B is non-zero.

For BCs2 with restrained circumferential displacements, the influence of the imperfection sign is not found due to the symmetry of imperfections.

Validation of numerical buckling results of isotropic cylindrical panels compressed according to different (force and kinematic) loading schemes was carried out. In general, different schemes of loading allow to accurately enough predict the load-deflection response of panels considered in known solutions and experiments. In the case of perfect panels, differences between loading schemes are negligible, while in the case of imperfections they are more significant and ought to be taken into account.

APPENDIX

In thin-walled FG structures such as plates, panels or shells, the volume fractions of ceramics V_c and metal V_m are described usually by a simple power law of distribution throughout the structure thickness t :

$$(A.1) \quad V_c(z) = (z/t + 0.5)^q, \quad V_m(z) = 1 - V_c(z).$$

According to the rule of mixture, the properties of the functionally graded material (Young's modulus, Poisson's ratio) can be expressed:

$$(A.2) \quad E(z) = E_m + (E_c - E_m) \left(\frac{z}{t} + \frac{1}{2} \right)^q, \quad \nu(z) = \nu_m + (\nu_c - \nu_m) \left(\frac{z}{t} + \frac{1}{2} \right)^q.$$

Using the CLPT, the stress and moment resultants (N, M) for FGM panel structures are defined as [15, 16, 20, 21]

$$(A.3) \quad \begin{Bmatrix} N \\ M \end{Bmatrix} = \begin{bmatrix} A & B \\ B & D \end{bmatrix} \begin{Bmatrix} \varepsilon \\ \kappa \end{Bmatrix},$$

where: A, B, D are extensional, coupling and bending stiffness matrices, respectively, and

$$(A.4) \quad \{\varepsilon\} = \begin{Bmatrix} \varepsilon_x \\ \varepsilon_y \\ 2\varepsilon_{xy} \end{Bmatrix}, \quad \{\kappa\} = \begin{Bmatrix} \kappa_x \\ \kappa_y \\ \kappa_{xy} \end{Bmatrix}.$$

Due to the presence of the non-trivial submatrix B , the coupling between extensional and bending deformations exists as it is in the case of non-symmetric laminated panels [16, 20, 21]. An extensional force results not only in extensional

deformations, but also in bending of the FGM panel. Moreover, such a panel cannot be subjected to the moment without suffering simultaneously from extension of the middle surface. The coupling between extension and bending follows from a combination of the geometry and FGM properties in that structure. The coupling affects strongly the constitutive equations and the boundary conditions that have a complex form, and the solution procedures become thereby difficult [15].

REFERENCES

1. BIRMAN V., BYRD L.W., *Modeling and analysis of functionally graded materials and structures*, Appl. Mech. Rev., **60**(5): 195–216, 2007.
2. LIEW K.M., ZHAO X., FERREIRA A.J.M., *A review of meshless methods for laminated and functionally graded plates and shells*, Composite Structures, **93**(8): 2031–2041, 2011.
3. JHA D.K., KANT T., SINGH R.K., *A critical review of recent research on functionally graded plates*, Composite Structures, **96**: 833–849, 2013.
4. SWAMINATHAN K., NAVEENKUMAR D.T., ZENKOUR A.M., CARRERA E., *Stress, vibration and buckling analyses of FGM plates – A state-of-the-art review*, Composite Structures, **120**: 10–31, 2015.
5. BIRMAN V., *Stability of functionally graded hybrid composite plates*, Compos. Eng., **7**(195): 913–921, 1997.
6. MA L.S., WANG T.J., *Relationships between axisymmetric bending and buckling solutions of FGM circular plates based on third-order plate theory and classical plate theory*, Int. J. Solids Struct., **41**(1): 85–101, 2004.
7. MOHAMMADI M., SAIDI A., JOMEHZADEH E., *Levy solution for buckling analysis of functionally graded rectangular plates*, Appl. Composite Materials, **17**(2): 81–93, 2010.
8. NADERI A., SAIDI A.R., *On pre-buckling configuration of functionally graded Mindlin rectangular plates*, Mech. Res. Commun., **37**(6): 535–538, 2010.
9. BATENI M., KIANI Y., ESLAMI M.R., *A comprehensive study on stability of FGM plates*, Int. J. Mech. Sci., **75**: 134–144, 2013.
10. NAEI M.H., MASOUMI A., SHAMEKHI A., *Buckling analysis of circular functionally graded material plate having variable thickness under uniform compression by finite-element method*, J. Mech. Eng. Sci., **221**(11): 1241–1247, 2017.
11. LEE C.Y., KIM J.H., *Hygrothermal postbuckling behavior of functionally graded plates*, Composite Structures, **95**: 278–282, 2013.
12. YANG J., SHEN H., *Non-linear analysis of functionally graded plates under transverse and in-plane loads*, Int. J. Non. Linear Mech., **38**(4): 467–482, 2003.
13. YANG J., LIEW K.M., KITIPORNCHAI S., *Imperfection sensitivity of the post-buckling behavior of higher-order shear deformable functionally graded plates*, Int. J. Solids Struct., **43**(17): 5247–5266, 2006.
14. HUI-SHEN S., *Functionally graded materials – Nonlinear analysis of plates and shells*, CRC Press, Taylor & Francis, London, 2009.

15. KOLAKOWSKI Z., MANIA R.J., GRUDZIECKI J., *Local unsymmetric postbuckling equilibrium path in thin FGM plate*, Eksploatacja i Niezawodność – Maintenance and Reliability, **17**(1): 135–142, 2015.
16. JONES R.M., *Mechanics of composite materials*, 2nd ed., Taylor & Francis, London, 1999.
17. KROLAK M., MANIA R.J. [Eds.], *Stability of Thin-Walled Plate Structures*, Monographs of TUL, pp. 131–153, 2011.
18. LYKHACHOVA O., KOLAKOWSKI Z., *Influence of the coupling submatrix B on the nonlinear stability of FG cylindrical panels subjected to compression*, TKI-2016, Warsaw, 2016.
19. LIEW K.M., LEI Z.X., YU J.L., ZHANG L.W., *Postbuckling of carbon nanotube-reinforced functionally graded cylindrical panels under axial compression using a meshless approach*, Comput. Methods Appl. Mech. Engrg., **268**: 1–17, 2014.
20. KOLAKOWSKI Z., KOWAL-MICHALSKA K. [Eds.], *Selected problems of instabilities in composite structures*, A Series of Monographs, TUL, Lodz 1995.
21. REDDY J.N., *Analysis of functionally graded plates*, Int. J. Numer. Meth. Eng., **47**: 663–684, 2000.
22. THORNBURGH R.P., HILBURGER M.W., *Identifying and characterizing discrepancies between test and analysis results of compression-loaded panels*, NASA/TM-2005-213932, 2005.
23. LYKHACHOVA O.V., *Numerical simulation of axially compressed cylindrical shells with circular cutouts*, Journal of Mechanics and Mechanical Engineering, **20**(3): 311–320, 2016.

Received February 1, 2017; accepted version August 28, 2017.
